Impurity-Induced Spin-Orbit Coupling in Graphene

A. H. Castro Neto[1] and F. Guinea[2]

[1]*Department of Physics, Boston University, 590 Commonwealth Avenue, Boston Massachusetts 02215, USA*
[2]*Instituto de Ciencia de Materiales de Madrid, CSIC, Cantoblanco E28049 Madrid, Spain*

We study the effect of impurities in inducing spin-orbit coupling in graphene. We show that the sp^3 distortion induced by an impurity can lead to a large increase in the spin-orbit coupling with a value comparable to the one found in diamond and other zinc-blende semiconductors. The spin-flip scattering produced by the impurity leads to spin scattering lengths of the order found in recent experiments. Our results indicate that the spin-orbit coupling can be controlled via the impurity coverage.

Since the discovery of graphene in 2004 [1] much has been written about its extraordinary charge transport properties [2,3], such as submicron electron mean-free paths, that derive from the specificity of the carbon σ-bonds against atomic substitution by extrinsic atoms. However, being an open surface, it is relatively easy to hybridize the graphene's p_z orbitals with impurities with direct consequences in its transport properties [4,5]. This capability for hybridization with external atoms, such as hydrogen (the so-called graphane), has been shown to be controllable and reversible [6] leading to new doors to control graphene's properties.

Much less has been said about the spin-related transport properties such as spin relaxation, although recent experiments show that the spin diffusion length scales [7,8] are much shorter than what one would expect from standard spin-orbit (SO) scattering mechanisms in a sp^2 bonded system [9]. In fact, atomic SO coupling in flat graphene is a very weak second order process since it affects the π orbitals only through virtual transitions into the deep σ bands [10–12]. Nevertheless, it would be very interesting if one could enhance SO interactions because of the prediction of the quantum spin Hall effect in the honeycomb lattice [13] and its relation to the field of topological insulators [14].

In this Letter we argue that impurities (adatoms), such as hydrogen, can lead to a strong enhancement of the SO coupling due to the lattice distortions that they induce. In fact, it is well known that atoms that hybridize directly with a carbon atom induce a distortion of the graphene lattice from sp^2 to sp^3 [15]. By doing that, the electronic energy is lowered and the path way to chemical reaction is enhanced. It is well established that in diamond [16], a purely sp^3 carbon bonded system, spin-orbit coupling plays an important role in the band structure since it is a first order effect, of the order of the atomic SO interaction, $\Delta_{SO}^{at} \approx$ 10 meV, in carbon [17]. Here we show that the impurity-induced sp^3 distortion of the flat graphene lattice lead to a significant enhancement of the SO coupling, explaining recent experiments [7,8] in terms of the Elliot-Yafet mechanism for spin relaxation [18,19] due to presence of

unavoidable environmental impurities in the experiment. Moreover, our predictions can be checked in a controllable way in graphane [6] by the control of the hydrogen coverage.

We assume that the carbon atom attached to an impurity is raised above the plane defined by its three carbon neighbors (see Fig. 1). The local orbital basis at the position of the impurity (which is assumed to be located at the origin, $\mathbf{R}_{i=0} = \mathbf{0}$) can be written as [20]:

$$|\pi_{i=0}\rangle = A|s\rangle + \sqrt{1 - A^2}|p_z\rangle,$$

$$|\sigma_{1,i=0}\rangle = \sqrt{\frac{1-A^2}{3}}|s\rangle - \frac{A}{\sqrt{3}}|p_z\rangle + \sqrt{\frac{2}{3}}|p_x\rangle,$$

$$|\sigma_{2,i=0}\rangle = \sqrt{\frac{1-A^2}{3}}|s\rangle - \frac{A}{\sqrt{3}}|p_z\rangle - \frac{1}{\sqrt{6}}|p_x\rangle + \frac{1}{\sqrt{2}}|p_y\rangle, \quad (1)$$

$$|\sigma_{3,i=0}\rangle = \sqrt{\frac{1-A^2}{3}}|s\rangle - \frac{A}{\sqrt{3}}|p_z\rangle - \frac{1}{\sqrt{6}}|p_x\rangle - \frac{1}{\sqrt{2}}|p_y\rangle,$$

where $|s\rangle$, and $|p_{x,y,z}\rangle$, are the local atomic orbitals. Notice that this choice of orbitals interpolates between the sp^2 configuration, $A = 0$, to the sp^3 configuration, $A = 1/2$. The angle θ between the new σ orbitals and the direction normal to the plane is $\cos(\theta) = -A/\sqrt{A^2 + 2}$. The energy of the state $|\pi_i\rangle$, ϵ_π, and the energy of the three degenerate states $|\sigma_{a,i}\rangle$, ϵ_σ ($a = 1, 2, 3$), are given by (see Fig. 2):

$$\epsilon_\pi(A) = A^2\epsilon_s + (1 - A^2)\epsilon_p, \quad (2)$$

$$\epsilon_\sigma(A) = (1 - A^2)\epsilon_s/3 + (2 + A^2)\epsilon_p/3, \quad (3)$$

where $\epsilon_s \approx -19.38$ eV ($\epsilon_p \approx -11.07$ eV) is the energy of the s (p) orbital [21]. At the impurity site one has $A \approx 1/2$ while away from the impurity $A = 0$.

The Hamiltonian of the problem can be written as $\mathcal{H} = \mathcal{H}_\pi + \mathcal{H}_\sigma + \delta\mathcal{H}$, where $\mathcal{H}_\pi$ ($\mathcal{H}_\sigma$) describes the π-band (σ-band) of flat graphene, and $\delta\mathcal{H}$ describes the *local* change in the hopping energies due to the presence of the impurity and sp^3 distortion:
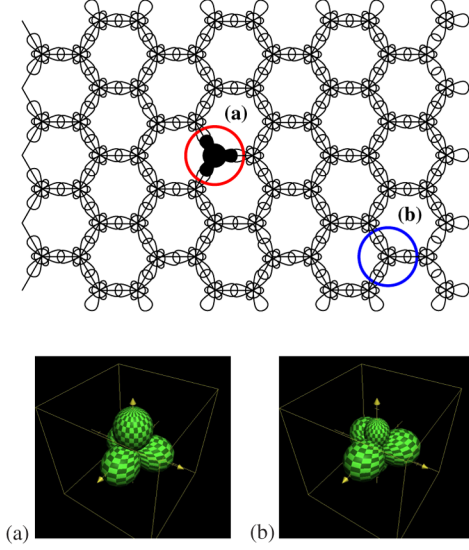
FIG. 1 (color online). Top: Top view of the graphene lattice with its orbitals. The orbitals associated with the impurity and lattice distortion are shown in solid black. (a) sp^3 orbital at impurity position; (b) sp^2 orbital of the flat graphene lattice.

$$\delta\mathcal{H} = \sum_{\alpha=\uparrow,\downarrow}\{\epsilon_I c_{I\alpha}^\dagger c_{I\alpha} + t_{C-I}c_{I\alpha}^\dagger c_{\pi\alpha0} + \delta\epsilon_\pi c_{\pi\alpha0}^\dagger c_{\pi\alpha0}$$
$$+ \delta\epsilon_\sigma \sum_{a=1,2,3} c_{\sigma_a\alpha0}^\dagger c_{\sigma_i\alpha0}$$
$$+ V_{\pi\sigma}c_{\pi\alpha0}^\dagger(c_{\sigma_1\alpha0} + c_{\sigma_2\alpha0} + c_{\sigma_3\alpha0}) + \text{H.c.}\}, \quad (4)$$

where

$$V_{\pi\sigma}(A) = A\sqrt{\frac{1-A^2}{3}}(\epsilon_s - \epsilon_p), \quad (5)$$

$c_{I,\alpha}$ ($c_{I,\alpha}^\dagger$) annihilates (creates) an electron at the impurity, and $c_{\pi\alpha i}$ ($c_{\sigma_a\alpha i}$) annihilates an electron at a carbon site in an orbital π (σ_a) at position $\mathbf{R}_i$ with spin α, ϵ_I is the electron energy in the impurity, and t_{C-I} the tunneling energy between the carbon and impurity, $\delta\epsilon_\pi(A) = \epsilon_\pi(A) - \epsilon_\pi(A=0)$, and $\delta\epsilon_\sigma(A) = \epsilon_\sigma(A) - \epsilon_\sigma(A=0)$. In (4) we have not included the change in the hopping between $\sigma_{a,0}$ orbitals (the change in energy due to the distortion is $-A^2(\epsilon_s - \epsilon_p)/3$) and the interatomic hopping terms. In this way, we have simplified the calculations and the interpretation of the results. The inclusion of the other terms do not modify our conclusions.

The atomic spin-orbit coupling, $\mathcal{H}_{SO}^{at} = \Delta_{SO}^{at}\mathbf{L}\cdot\mathbf{S}$, induces transitions between p orbitals of different spin projection [10]. In flat graphene ($A=0$), it leads to transitions between the π and σ bands. The change in the ground state energy in this case is rather small and given by $(\Delta_{SO}^{at})^2/[\epsilon_\pi(A=0) - \epsilon_\sigma(A=0)] \approx 10^{-2}$ meV [10]. However, the perturbation described by (4) leads to a direct local hybridization $V_{\pi\sigma}$ between the π and σ bands that modifies the effective SO coupling acting on the π electrons. The propagator of π electrons from position $\mathbf{R}_i$ with
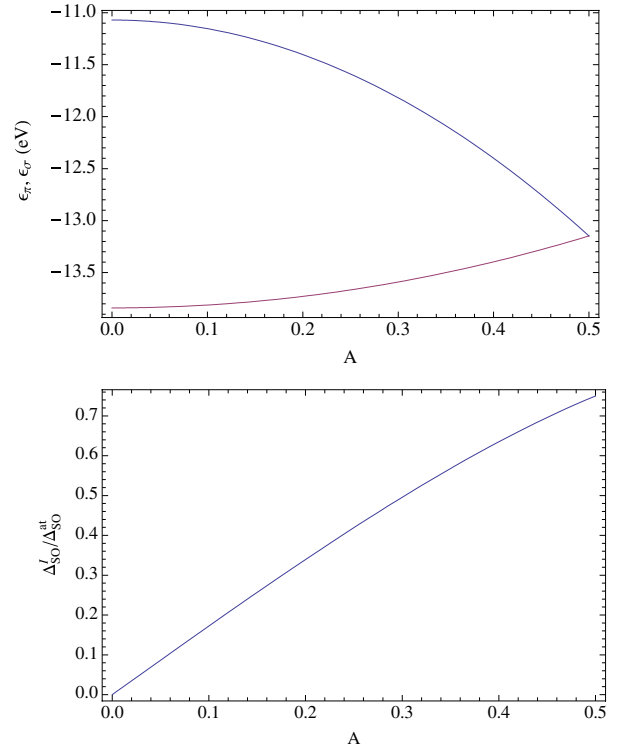
FIG. 2 (color online). Top: Energy (in eV) of the π (blue) and σ (red) bands as a function of A according to (3). Bottom: Relative value of the SO coupling at the impurity site relative to the atomic value in carbon as a function of A according to (8).

spin α to $\mathbf{R}_j$ with spin β can be written as

$$\langle\pi_{i,\alpha}|(\epsilon - \mathcal{H})^{-1}|\pi_{j,\beta}\rangle \approx \langle\pi_{i,\alpha}|(\epsilon - \mathcal{H}_\pi)^{-1}|\pi_{0,\alpha}\rangle\langle\pi_{0,\alpha}|$$
$$\times \delta\mathcal{H}|\bar{\sigma}_{0,\alpha}\rangle\langle\bar{\sigma}_{0,\alpha}|$$
$$\times (\epsilon - \mathcal{H}_\sigma)^{-1}|\bar{\bar{\sigma}}_{k,\alpha}\rangle\langle\bar{\bar{\sigma}}_{k,\alpha}|$$
$$\times \mathcal{H}_{SO}^{at}|\pi_{k,\beta}\rangle\langle\pi_{k,\beta}|$$
$$\times (\epsilon - \mathcal{H}_\pi)^{-1}|\pi_{j,\beta}\rangle, \quad (6)$$

where $|\bar{\sigma}_{0,\alpha}\rangle = [|\sigma_{10,\alpha}\rangle + |\sigma_{20,\alpha}\rangle + |\sigma_{30,\alpha}\rangle]/\sqrt{3}$ and $\bar{\bar{\sigma}}_{j,\alpha}\rangle = [|\sigma_{1j,\alpha}\rangle + e^{i\phi}|\sigma_{2j,\alpha}\rangle + e^{2i\phi}|\sigma_{3j,\alpha}\rangle]/\sqrt{3}$, where $\phi = 2\pi/3$. The propagator in (6) can be understood as arising from an effective nonlocal SO coupling within the π band which goes as

$$\Delta_{SO}^I(0, i) \approx V_{\pi\sigma}\langle\bar{\sigma}_{0,\alpha}|(\epsilon - \mathcal{H}_\sigma)^{-1}|\bar{\bar{\sigma}}_{i,\alpha}\rangle\Delta_{SO}^{at}, \quad (7)$$

which allows us to estimate the local value of the SO coupling as

$$\frac{\Delta_{SO}^I(A)}{\Delta_{SO}^{at}} \approx A\sqrt{3(1-A^2)}. \quad (8)$$

As shown in Fig. 2 the value of the SO coupling depends on the angle (i.e., the value of A) associated with the distortion of the carbon atom away from the graphene plane. Notice that for the sp^2 case ($A=0$) this term vanishes indicating that SO only contributes in second order in Δ_{SO}^{at}, while for
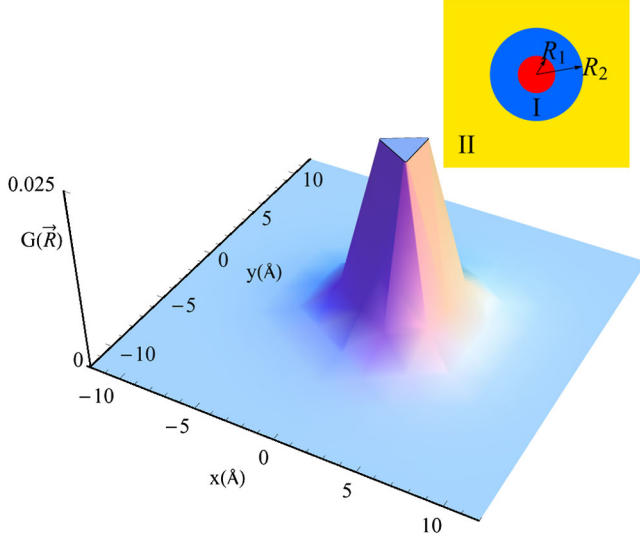
FIG. 3 (color online). Decay of the σ band propagator which determines the effective spin-orbit coupling as function of the distance to the carbon atom with partial sp^3 coordination. The model for the σ band is discussed in [10]. The inset shows the model used to study the scattering process around an atom with partial sp^3 coordination (see text for details).

the sp^3 case ($A = 1/2$), the SO coupling is approximately 75% of the atomic value (≈ 7 meV).

The dependence on the distance from the location of the hydrogen atom is determined by the Green's function $G_\sigma(0, \mathbf{R}_j) = \langle \bar{\sigma}_0 | (\epsilon - \mathcal{H}_\sigma)^{-1} | \bar{\bar{\sigma}}_j \rangle$ whose Fourier transform is $G_\sigma(\epsilon, \mathbf{k}) = \sum_l [(\bar{\alpha}_\mathbf{k}^l)^* \bar{\alpha}_\mathbf{k}^l (\epsilon - \epsilon_\mathbf{k}^l)^{-1}$, where the sum over l includes the σ bands, $\bar{\alpha}_\mathbf{k}^l$ gives the overlap

between the orbital combination $\bar{\sigma}$ and the wave functions of the σ bands, and $\bar{\bar{\alpha}}_\mathbf{k}^l$ gives the corresponding value for $\bar{\bar{\sigma}}$. The Fourier transform of this function, $G(\vec{R}, \epsilon)$, evaluated using the simplified model in [10] at the Dirac energy, $\epsilon = 0$, is shown in Fig. 3. This function decays rapidly as a function of the distance to the central atom.

Based on the previous results we can now calculate the effect of the impurity-induced SO coupling in the transport properties. First, we linearize the π band around the K and K' points in the Brillouin zone and find the 2D Dirac spectrum [3]: $\epsilon_{\pm, \mathbf{k}} = \pm v_F k$ where v_F ($\approx 10^6$ m/s) is the Fermi-Dirac velocity. In this long wavelength limit the impurity potential induced by (7) has cylindrical symmetry and we can use a decomposition of the wave function in terms of radial harmonics [22–26]. A similar analysis, for a system with SO interaction in the bulk has been studied in Ref. [9]. We assume that the sp^3 distortion of the lattice occurs in a region of radius R_2 ($\approx 2a - 3a$). In this region the wave functions are modified by the SO coupling and for $r > R_2$ the system is purely sp^2 bonded. At $r = R_2$ the wave function is continuous. Since we are going to work with the low energy effective theory which relies on the expansion of the energy around the K (K') points, we have to introduce a short distance cutoff, R_1 ($\approx a$). We assume that the wave function vanishes for distances $r \leq R_1$ [27]. Because of the extrinsic nature of the impurity we describe it by a Rashba-like SO interaction that exists in the region $R_1 \leq r \leq R_2$ (region I), and there is neither potential nor spin-orbit interaction for $r > R_2$, region II. A sketch of this geometry is shown in Fig. 3.

The wave functions in region I can be written as a superposition of angular harmonics:

$$\Psi_n(r, \theta) \equiv A_+ \left[\begin{pmatrix} c_+ J_n(k_+ r) e^{in\theta} \\ ic_- J_{n+1}(k_+ r) e^{i(n+1)\theta} \end{pmatrix} |\uparrow\rangle + \begin{pmatrix} ic_- J_{n+1}(k_+ r) e^{i(n+1)\theta} \\ -c_+ J_{n+2}(k_+ r) e^{i(n+2)\theta} \end{pmatrix} |\downarrow\rangle \right] + B_+ \left[\begin{pmatrix} c_+ Y_n(k_+ r) e^{in\theta} \\ ic_- Y_{n+1}(k_+ r) e^{i(n+1)\theta} \end{pmatrix} |\uparrow\rangle \right.$$

$$+ \begin{pmatrix} ic_- Y_{n+1}(k_+ r) e^{i(n+1)\theta} \\ -c_+ Y_{n+2}(k_+ r) e^{i(n+2)\theta} \end{pmatrix} |\downarrow\rangle \right] + A_- \left[\begin{pmatrix} c'_- J_n(k_- r) e^{i\theta} \\ ic'_+ J_{n+1}(k_- r) e^{i(n+1)\theta} \end{pmatrix} |\uparrow\rangle - \begin{pmatrix} ic'_+ J_{n+1}(k_- r) e^{i(n+1)\theta} \\ -c'_- J_{n+2}(k_- r) e^{i(n+2)\theta} \end{pmatrix} |\downarrow\rangle \right]$$

$$+ B_- \left[\begin{pmatrix} c'_- Y_n(k_- r) e^{in\theta} \\ ic'_+ Y_{n+1}(k_- r) e^{i(n+1)\theta} \end{pmatrix} |\uparrow\rangle - \begin{pmatrix} ic'_+ Y_{n+1}(k_- r) e^{i(n+1)\theta} \\ -c'_- Y_{n+2}(k_- r) e^{i(n+2)\theta} \end{pmatrix} |\downarrow\rangle \right] \tag{9}$$

where $|\uparrow\rangle$ and $|\downarrow\rangle$ are the spin states. The functions $J_n(x)$, $Y_n(x)$ are Bessel functions of order n, and

$$\epsilon = \pm \Delta_{SO}^I / 2 + \sqrt{v_F^2 k_\pm^2 + (\Delta_{SO}^I / 2)^2}, \tag{10}$$

$$c_\pm = \sqrt{1/2 \pm \Delta_{SO}^I / (4 \sqrt{v_F^2 k_+^2 + (\Delta_{SO}^I / 2)^2})}, \tag{11}$$

$$c'_\pm = \sqrt{1/2 \pm \Delta_{SO}^I / (4 \sqrt{v_F^2 k_-^2 + (\Delta_{SO}^I / 2)^2})}, \tag{12}$$

ϵ is the energy of the scattered electron [$k_\pm$ is defined through (10)].

The wave functions outside the region affected by the impurity, $r > R_2$, can be written as

$$\Psi_n(r, \theta) \equiv \begin{pmatrix} J_n(kr) e^{in\theta} \\ iJ_{n+1}(kr) e^{i(n+1)\theta} \end{pmatrix} |\uparrow\rangle$$

$$+ C_\uparrow \begin{pmatrix} Y_n(kr) e^{in\theta} \\ iY_{n+1}(kr) e^{i(n+1)\theta} \end{pmatrix} |\uparrow\rangle$$

$$+ C_\downarrow \begin{pmatrix} Y_{n+1}(kr) e^{i(n+1)\theta} \\ iY_{n+2}(kr) e^{i(n+2)\theta} \end{pmatrix} |\downarrow\rangle \tag{13}$$

and $\epsilon = v_F k$. The boundary conditions at $r = R_1$ and $r = R_2$ lead to the six equations, whose solutions allow us to
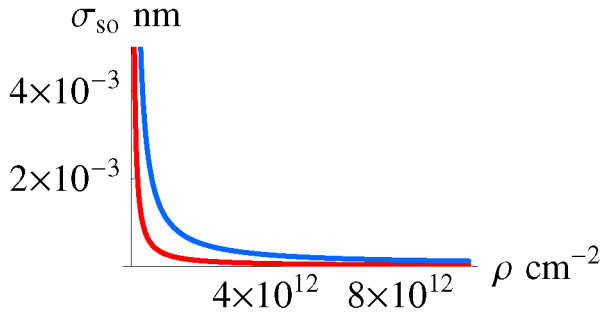
FIG. 4 (color online).   Cross section for a spin-flip process for a defect as described in the text. The parameters used are $R_1 = 1$ Å, $R_2 = 2$ Å, and $\Delta_{SO}^l = 1$ meV (blue) and $\Delta_{SO}^l = 2$ meV (red).

obtain the coefficients $A_\pm$, $B_\pm$, $C_\uparrow$ and $C_\downarrow$. In the absence of the SO interaction, we have $A_+ = A_-$, $B_+ = B_-$, $C_\downarrow = 0$ and $C_\uparrow = -J_n(kR_1)/Y_n(kR_1)$.

We show in Fig. 4 the results for the cross section for spin-flip processes, determined by $|C_\downarrow|^2/k_F$ [we assume $A \approx 0.1$–0.2 in accordance with *ab initio* calculations [15] and obtain Δ_{SO}^l from Eq. (8)]. The main contribution arises from the $n = 0$ channel. For comparison, the elastic cross section, calculated in the same way, is $\sigma_{el} \approx k_F^{-1}$. This is about 3 orders of magnitude larger than the spin-flip cross section due to the spin-orbit coupling. Hence, the spin relaxation length is 10^3 times the elastic mean-free path [9]. We obtain a spin relaxation length of 1 μm, in reasonable agreement with the experimental results in Ref. [7]. This value depends quadratically on $\Delta_{SO}^l(A)$. For a finite, but small, concentration of impurities, our results scale with the impurity concentration and hence the spin-flip processes should increase roughly linearly with impurity coverage in transport experiments in systems like graphane [6].

In summary, we have shown that the impurity-induced, lattice-driven, SO coupling in graphene can be of the order of the atomic spin-orbit coupling and comparable to what is found in diamond and zinc-blende semiconductors. The value of the SO coupling depends on how much the carbon atom which is hybridized with the impurity displaces from the plane inducing a sp^3 hybridization. We have calculated the spin-flip cross section due to SO coupling for the impurity and shown that it agrees with recent experiments. This result indicates that there are substantial amounts of hybridized impurities in graphene, even under ultraclean high vacuum conditions. Experiments where the impurity coverage is well controlled can provide a ''smoking-gun'' test of our predictions.

[1] K. S. Novoselov *et al.*, Science **306**, 666 (2004).
[2] A. K. Geim and K. S. Novoselov, Nature Mater. **6**, 183 (2007).
[3] A. H. Castro Neto *et al.*, Rev. Mod. Phys. **81**, 109 (2009).
[4] J. H. Chen *et al.*, Nature Phys. **4**, 377 (2008).
[5] P. Blake *et al.*, arXiv:0810.4706.
[6] D. C. Elias *et al.*, Science **323**, 610 (2009).
[7] N. Tombros *et al.*, Nature (London) **448**, 571 (2007).
[8] N. Tombros *et al.*, Phys. Rev. Lett. **101**, 046601 (2008).
[9] D. Huertas-Hernando, F. Guinea, and A. Brataas, arXiv:0812.1921.
[10] D. Huertas-Hernando, F. Guinea, and A. Brataas, Phys. Rev. B **74**, 155426 (2006).
[11] H. Min, J. E. Hill, N. Sinitsyn, B. Sahu, L. Kleinman, and A. MacDonald, Phys. Rev. B **74**, 165310 (2006).
[12] Y. Yao *et al.*, Phys. Rev. B **75**, 041401(R) (2007).
[13] C. L. Kane and E. J. Mele, Phys. Rev. Lett. **95**, 226801 (2005).
[14] C. Kane and E. Mele, Science **314**, 1692 (2006).
[15] E. J. Duplock, M. Scheffler, and P. J. Lindan, Phys. Rev. Lett. **92**, 225502 (2004).
[16] P. Y. Yu and M. Cardona, *Fundamentals of Semiconductors: Physics and Materials Properties* (Springer, New York, 2005).
[17] J. Serrano, M. Cardona, and T. Ruf, Solid State Commun. **113**, 411 (2000).
[18] P. G. Elliot, Phys. Rev. **96**, 266 (1954).
[19] Y. Yafet, in *Solid State Physics*, edited by F. Seitz and D. Turnbull (Academic, New York, 1963), Vol. 13.
[20] L. Pauling, *The Nature of the Chemical Bond* (Cornell University Press, Ithaca, NY, 1972).
[21] W. A. Harrison, *Solid State Theory* (Dover, New York, 1980).
[22] P. M. Ostrovsky, I. V. Gornyi, and A. D. Mirlin, Phys. Rev. B **74**, 235443 (2006).
[23] M. Hentschel and F. Guinea, Phys. Rev. B **76**, 115407 (2007).
[24] D. S. Novikov, Phys. Rev. B **76**, 245435 (2007).
[25] M. I. Katsnelson and K. S. Novoselov, Solid State Commun. **143**, 3 (2007).
[26] F. Guinea, J. Low Temp. Phys. **153**, 359 (2008).
[27] V. M. Pereira *et al.*, Phys. Rev. Lett. **96**, 036801 (2006).